Available online at www.sciencedirect.com

SCIENCE DIRECT®

Virology 319 (2004) 141–151

VIROLOGY

www.elsevier.com/locate/yviro

Characterization of bacteriophage KVP40 and T4 RNA ligase 2☆

Shenmin Yin,[a] C. Kiong Ho,[a] Eric S. Miller,[b] and Stewart Shuman[a,*]

[a] *Molecular Biology Program, Sloan-Kettering Institute, New York, NY 10021, USA*

[b] *Department of Microbiology, North Carolina State University, Raleigh, NC 27695-7615, USA*

Received 25 September 2003; returned to author for revision 31 October 2003; accepted 31 October 2003

Abstract

Bacteriophage T4 RNA ligase 2 (Rnl2) exemplifies a subfamily of RNA strand-joining enzymes that includes the trypanosome RNA editing ligases. A homolog of T4 Rnl2 is encoded in the 244-kbp DNA genome of vibriophage KVP40. We show that the 335-amino acid KVP40 Rnl2 is a monomeric protein that catalyzes RNA end-joining through ligase–adenylate and RNA–adenylate (AppRNA) intermediates. In the absence of ATP, pre-adenylated KVP40 Rnl2 reacts with an 18-mer 5′ -PO_4 single-strand RNA (pRNA) to form an 18-mer RNA circle. In the presence of ATP, Rnl2 generates predominantly AppRNA. Isolated AppRNA can be circularized by KVP40 Rnl2 in the absence of ATP. The reactivity of phage Rnl2 and the distribution of the products are affected by the length of the pRNA substrate. Whereas 18-mer and 15-mer pRNAs undergo intramolecular sealing by T4 Rnl2 to form monomer circles, a 12-mer pRNA is ligated intermolecularly to form dimers, and a 9-mer pRNA is unreactive. In the presence of ATP, the 15-mer and 12-mer pRNAs are converted to AppRNAs, but the 9-mer pRNA is not. A single 5′ deoxynucleotide substitution of an 18-mer pRNA substrate has no apparent effect on the 5′ adenylation or circularization reactions of T4 Rnl2. In contrast, a single deoxyribonucleoside at the 3′ terminus strongly and selectively suppresses the sealing step, thereby resulting in accumulation of high levels of AppRNA in the absence of ATP. The ATP-dependent "capping" of RNA with AMP by Rnl2 is reminiscent of the capping of eukaryotic mRNA with GMP by GTP:RNA guanylyltransferase and suggests an evolutionary connection between bacteriophage Rnl2 and eukaryotic RNA capping enzymes.

Keywords: Bacteriophage; KVP40; T4 RNA ligase 2

Introduction

Bacteriophage T4 encodes two RNA strand-joining enzymes, named RNA ligase 1 (Rnl1) and RNA ligase 2 (Rnl2), which exemplify different branches of the RNA ligase enzyme family. T4 Rnl1 was discovered in 1972 and is the founding member of the RNA-specific polynucleotide ligase family (Silber et al., 1972). The function of Rnl1 in vivo is to repair a break in the anticodon loop of *Escherichia coli* $tRNA^{Lys}$ triggered by phage activation of a host-encoded anticodon nuclease (Amitsur et al., 1987). Rnl1-like ligases are few in number and they have a narrow phylogenetic distribution. The Rnl1-like proteins include a putative RNA ligase/polynucleotide kinase of *Autographa californica* nucleopolyhedrovirus (AcNPV, a baculovirus) and the tRNA ligases of fungi (Baymiller et al., 1994; Durantel et al., 1998; Phizicky et al., 1986; Sawaya et al., in press). T4 Rnl2 typifies a separate subfamily (Ho and Shuman, 2002) that includes the RNA editing ligases of *Trypanosoma* and *Leishmania* (McManus et al., 2001; Rusche et al., 2001; Schnaufer et al., 2001), putative RNA ligases encoded by eukaryotic viruses (baculoviruses and an entomopoxvirus), and putative RNA ligases encoded by many species of archaea. Thus, the Rnl2-like ligases are present in all three phylogenetic domains. The function of T4 Rnl2 during phage infection is unknown.

RNA ligases join 3′ -OH and 5′ -PO_4 RNA termini through a series of three nucleotidyl transfer steps (Cranston et al., 1974; Sugino et al., 1977; Uhlenbeck and Gumport, 1982). Step 1 is the reaction of ligase with ATP to form a covalent ligase-(lysyl-N)–AMP intermediate and pyrophosphate. In step 2, the AMP is transferred from ligase–adenylate to the 5′ -PO_4 RNA end to form an RNA–adenylate intermediate (AppRNA). In step 3, attack by an RNA 3′ -OH on the RNA–adenylate seals the two ends via a phosphodiester bond and releases AMP. The active site

☆ Supported by NIH Grant GM63611.

* Corresponding author. Molecular Biology Program, Memorial Sloan-Kettering Cancer Center, 1275 York Avenue, New York, NY 10021. Fax: +1-212-717-3623.

E-mail address: s-shuman@ski.mskcc.org (S. Shuman).

0042-6822/$ - see front matter © 2003 Published by Elsevier Inc.
doi:10.1016/j.virol.2003.10.037

lysines of Rnl1 and Rnl2 are located within a conserved sequence element Kx[D/N/H]G (motif I) that defines a superfamily of covalent nucleotidyl transferases, which includes DNA ligases and mRNA capping enzymes (Shuman and Schwer, 1995; Thogersen et al., 1985; Tomkinson et al., 1991; Xu et al., 1990). DNA ligases and capping enzymes share a common tertiary structure composed of five conserved motifs (I, III, IIIa, IV, and V) that contain amino acid side chains responsible for nucleotide binding and catalysis (Fabrega et al., 2003; Håkansson et al., 1997; Lee et al., 2000; Odell et al., 2000; Subramanya et al., 1996;) (see Fig. 1). It has been suggested that DNA ligases and capping enzymes evolved from a common ancestral nucleotidyl transferase, possibly from an ancient RNA strand-joining enzyme (Shuman, 2000). An intriguing question is whether the ancestral RNA strand-joining enzyme resembled the Rnl1-like or Rnl2-like branches extant today.

Although there is no atomic structure available for any RNA ligase, comparisons of proteins sequences and the results of site-directed mutagenesis suggest a closer relationship of capping enzymes to T4 Rnl2 than to T4 Rnl1 (Wang et al., 2003; Yin et al., 2003). The primary

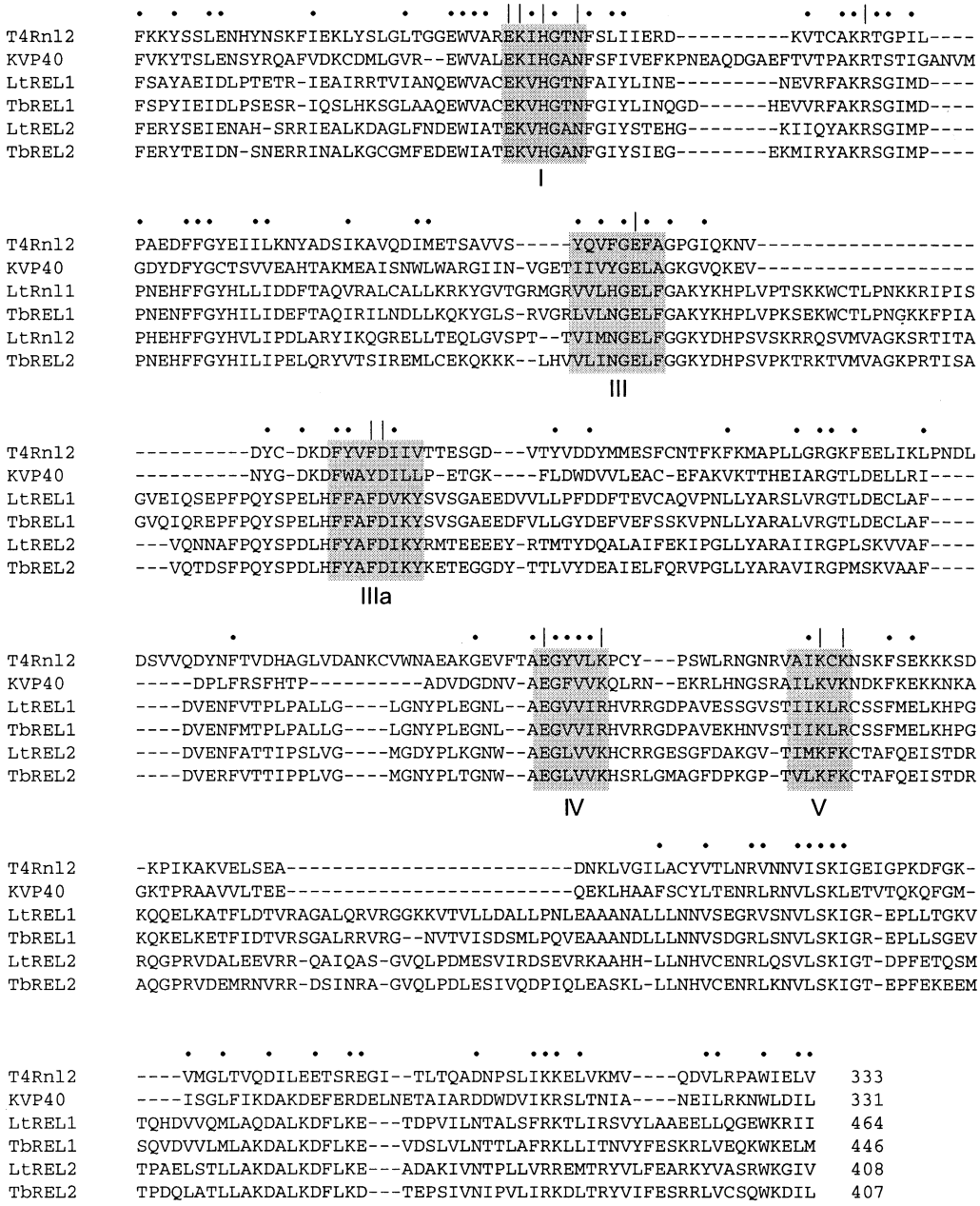

Fig. 1. Rnl2 subfamily of RNA ligases. The amino acid sequences of T4 and KVP40 Rnl2 are aligned to the sequences of RNA editing ligases 1 and 2 of *Trypanosoma brucei* and *Leishmania tarentolae*. Nucleotidyl transferase motifs I, III, IIIa, IV, and V are highlighted in shaded boxes. Positions of T4 Rnl2 that were shown by mutational analysis to be essential for Rnl2 activity are indicated by |. Positions of side chain identity/similarity in all six aligned proteins are indicated by dots (•).

structures of the Rnl1-like and Rnl2-like ligases are themselves quite dissimilar, with the only shared features being the presence of three of the nucleotidyl transferase motifs (I, IV, and V) that comprise the NMP-binding site of DNA ligases and RNA capping enzymes. In contrast, T4 Rnl2 has all five of the motifs that comprise the nucleotidyl transferase domain of capping enzymes and DNA ligases, and mutational analysis of T4 Rnl2 has pinpointed 12 amino acids within these motifs of T4 Rnl2 that are essential for RNA ligase activity (indicated by | over the sequence alignment in Fig. 1) (Ho and Shuman, 2002; Yin et al., 2003).

Initial biochemical characterization of T4 Rnl2 revealed an interesting effect of ATP, whereby reaction of Rnl2 with 5′ -PO_4 single-strand RNA in the presence of ATP resulted in the accumulation of high levels of AppRNA (Ho and Shuman, 2002). This trapping effect does not occur, or is much less marked, with T4 Rnl1 (Sugino et al., 1978). Note that the adenylated polynucleotide intermediate in the ligase reaction is chemically similar to the GpppRNA product of the eukaryotic mRNA capping reaction. This raises the prospect that T4 Rnl2 may play a role in RNA 5′ end modification, in addition to, or instead of, a putative function in RNA repair.

As a means to study the generality of the AMP-capping reaction seen with T4 Rnl2, we sought to identify and characterize new members of the Rnl2-like protein family. The recently completed genome sequence of the T4-like vibriophage KVP40 (Miller et al., 2003a) revealed a predicted 335-aa gene product with 35% identity to the 334-aa T4 Rnl2 polypeptide (Fig. 1). The conservation of Rnl2 in KVP40 is remarkable given that only 26% of the predicted KVP40 proteins have homologs in phage T4 and only 36% of T4 proteins have homologs in KVP40 (Miller et al., 2003a,b). The putative KVP40 Rnl2 contains the nucleotidyl transferase motifs (highlighted in boxes in Fig. 1) and its similarity to T4 Rnl2 and kinetoplastid RNA editing ligases extends throughout the entire length of the KVP40 polypeptide. (Residues conserved in all of the aligned proteins are indicated by · over the sequence in Fig. 1.) Here we have produced the KVP40 protein in *E. coli*, purified it, and characterized its physical and functional properties. We find that KVP40 Rnl2, like the T4 ortholog, caps single-stranded RNAs with AMP in the presence of ATP. We further characterize the phage T4 Rnl2 enzyme with respect to the effects of RNA strand length and terminal pentose sugar composition on the polynucleotide ligation and 5′ adenylylation reactions.

Results

Recombinant KVP40 Rnl2

We expressed KVP40 Rnl2 in *E. coli* as a His_{10}-tagged fusion and purified the 42-kDa recombinant protein from a soluble bacterial extract by adsorption to Ni–agarose and step-elution with imidazole (Fig. 2A). The 200-mM imidazole fraction was used for further characterization of KVP40 Rnl2. The adenylyltransferase activity of KVP40 Rnl2 was evinced by label transfer from [α-^{32}P]ATP to the Rnl2 polypeptide to form a covalent enzyme–adenylate adduct

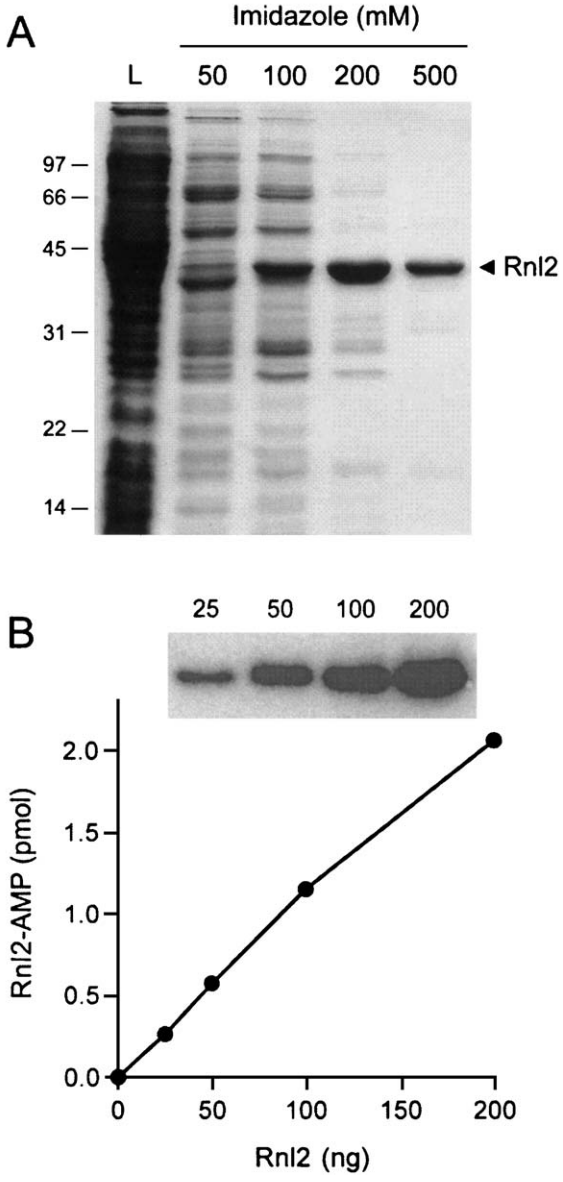

Fig. 2. Purification and adenylyltransferase activity of KVP40 Rnl2. (A) Aliquots (20 μl) of the soluble lysate of isopropyl-β-D-thiogalactoside (IPTG)-induced bacteria (L) and the indicated imidazole eluate fractions were analyzed by SDS-PAGE. The gel was stained with Coomassie blue dye. The positions and sizes (kDa) of marker polypeptides are shown on the *left*. (B) Adenylyltransferase reaction mixtures (20 μl) containing 50 mM Tris–HCl (pH 7.0), 5 mM DTT, 3 mM $MgCl_2$, 20 μM [α-^{32}P]ATP, and 25, 50, 100, or 200 ng of Rnl2 (i.e., 0.6, 1.3, 2.5, or 5 pmol Rnl2) were incubated for 5 min at 37°C. The reactions were quenched with SDS and the products were resolved by SDS-PAGE. An autoradiograph of the gel showing the protein–[^{32}P]AMP adduct is included above a plot of the yield of Rnl2–AMP versus input Rnl2 protein.

(Fig. 2B). The extent of Rnl2–AMP complex formation varied linearly with the amount of input Rnl2 (Fig. 2B). From the slope of the titration curve, we calculated that ~40% of the purified Rnl2 protein was adenylated with ^{32}P-AMP in vitro.

The native size of KVP40 Rnl2 was gauged by sedimentation through a 15–30% glycerol gradient. Marker proteins catalase (248 kDa), BSA (66 kDa), and cytochrome *c* (13 kDa) were included as internal standards. The Rnl2 polypeptide sedimented as a single discrete peak between BSA and cytochrome *c* (Fig. 3A). The adenylyltransferase activity profile paralleled the sedimentation profile of the Rnl2 polypeptide (Fig. 3B). We surmise that Rnl2 is a monomer in solution.

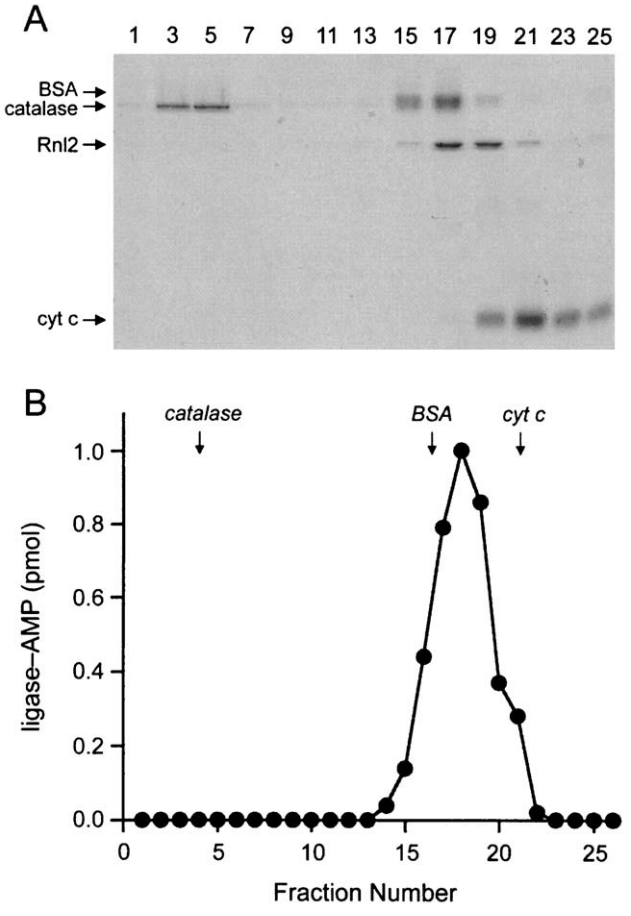

Fig. 3. Glycerol gradient sedimentation of KVP40 Rnl2. An aliquot (50 μg) of Rnl2 was mixed with 50 μg each of catalase, BSA, and cytochrome *c* and the mixture was applied to a 4.8-ml 15–30% glycerol gradient containing 50 mM Tris–HCl (pH 8.0), 2 mM DTT, 250 mM NaCl, and 0.1% Triton X-100. The gradient was centrifuged at 50,000 rpm for 18 h at 4°C in a Beckman SW50 rotor. Fractions were collected from the bottom of the tube. (A) Aliquots (20 μl) of odd numbered fractions were analyzed by SDS-PAGE. The Coomassie blue-stained gel is shown. The identities of the polypeptides are indicated on the *left*. (B) Aliquots (1 μl) of the glycerol gradient fraction were assayed for adenylyltransferase activity. The activity profile is shown. The positions of the peak fractions of catalase, BSA, and cytochrome *c* are indicated by arrows.

Characterization of the adenylyltransferase reaction of KVP40 Rnl2

The adenylyltransferase activity displayed a bell-shaped pH profile with an optimum at pH 7.0 (Fig. 4A). Activity was virtually nil at pH ≤ 5.0 or ≥ 9.5. KVP40 Rnl2 required a divalent cation cofactor to form the covalent AMP adduct. $MgCl_2$ supported optimal activity at 0.5–3 mM concentration (Fig. 4B). $MnCl_2$ supported optimal activity over a narrow range, 0.0625–0.125 mM, and activity declined steadily as manganese concentration was increased from 0.25 to 5 mM (Fig. 4B). The yield of Rnl2–AMP complex as a function of ATP concentration reached saturation at 20 μM (Fig. 4C).

RNA ligase activity

KVP40 Rnl2 was reacted with a 5′ ^{32}P-labeled 18-mer RNA oligonucleotide and magnesium in the presence or absence of 1 mM ATP. In both cases, Rnl2 formed new radiolabeled RNAs; however, the distribution of the products varied dramatically depending on whether ATP was present. When ATP was included, the predominant RNA product migrated ~1-nt slower than the input 18-mer strand (Fig. 5A). This species corresponded to the RNA–adenylate (AppRNA) generated by AMP transfer from Rnl2–AMP to the 5′ end of the input 18-mer RNA (Fig. 5C). In the absence of ATP, the major product, which migrated ~2-nt faster than the input 18-mer strand, corresponded to a covalently closed 18-mer circle formed by intramolecular ligation. Ligation in the absence of added ATP reflects the presence of pre-formed ligase–adenylate in the enzyme preparation.

The formation of AppRNA and circular RNA products with or without ATP is plotted in Fig. 6 as a function of input Rnl2. From the titration curve of the ATP-independent circularization reaction, we calculated that approximately one-sixth of the Rnl2 preparation was catalytically competent Rnl2–AMP (Fig. 6, right panel). In the presence of ATP, about 0.4 molecules of AppRNA were formed per input enzyme and ~80% of the input pRNA was adenylated at saturating levels of enzyme (Fig. 6, left panel). The likely explanation for the ATP effect in promoting accumulation of AppRNA is that KVP40 Rnl2 is prone to dissociate from the newly formed RNA–adenylate product of step 2 and that an immediate reaction with ATP to form ligase–adenylate precludes it from rebinding to the RNA–adenylate for subsequent catalysis of strand joining. Similar ATP trapping effects leading to the accumulation of high levels of AppRNA have been observed for T4 Rnl2 (Ho and Shuman, 2002). The experiment in Fig. 5D shows a smooth transition from circular product to AppRNA product as the ATP concentration was increased. The ATP concentration dependence of the trapping of RNA–adenylate roughly parallels the ATP concentration dependence of ligase–adenylate formation.

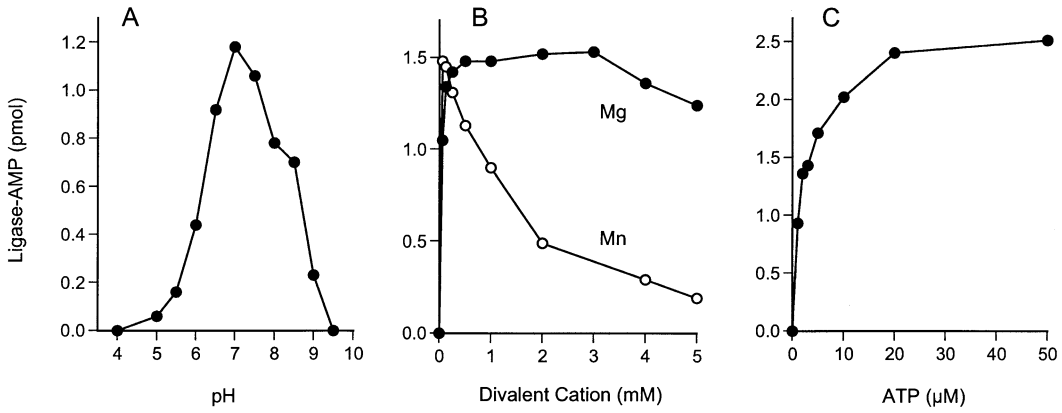

Fig. 4. Characterization of the KVP40 Rnl2 adenylyltransferase reaction. (A) pH dependence. Reaction mixtures (20 μl) containing 50 mM buffer (either Tris–acetate pH 4.0, 5.0, 5.5, 6.0, or 6.5 or Tris–HCl pH 7.0, 7.5, 8.0, 8.5, 9.0, or 9.5), 5 mM DTT, 3 mM $MgCl_2$, 20 μM [α-^{32}P]ATP, and 200 ng (5 pmol) Rnl2 were incubated for 5 min at 37°C. The extent of Rnl2–AMP formation is plotted as a function of pH. (B) Divalent cation dependence. Reaction mixtures (20 μl) containing 50 mM Tris–HCl (pH 7.0), 5 mM DTT, 20 μM [α-^{32}P]ATP, 200 ng Rnl2, and $MgCl_2$ or $MnCl_2$ as specified were incubated for 5 min at 37°C. Rnl2–AMP formation is plotted as a function of divalent cation concentration. (C) ATP dependence. Reaction mixtures (20 μl) containing 50 mM Tris–HCl (pH 7.0), 5 mM DTT, 3 mM $MgCl_2$, 200 ng Rnl2, and [α-^{32}P]ATP as specified were incubated for 5 min at 37°C. Rnl2–AMP formation is plotted as a function of ATP concentration.

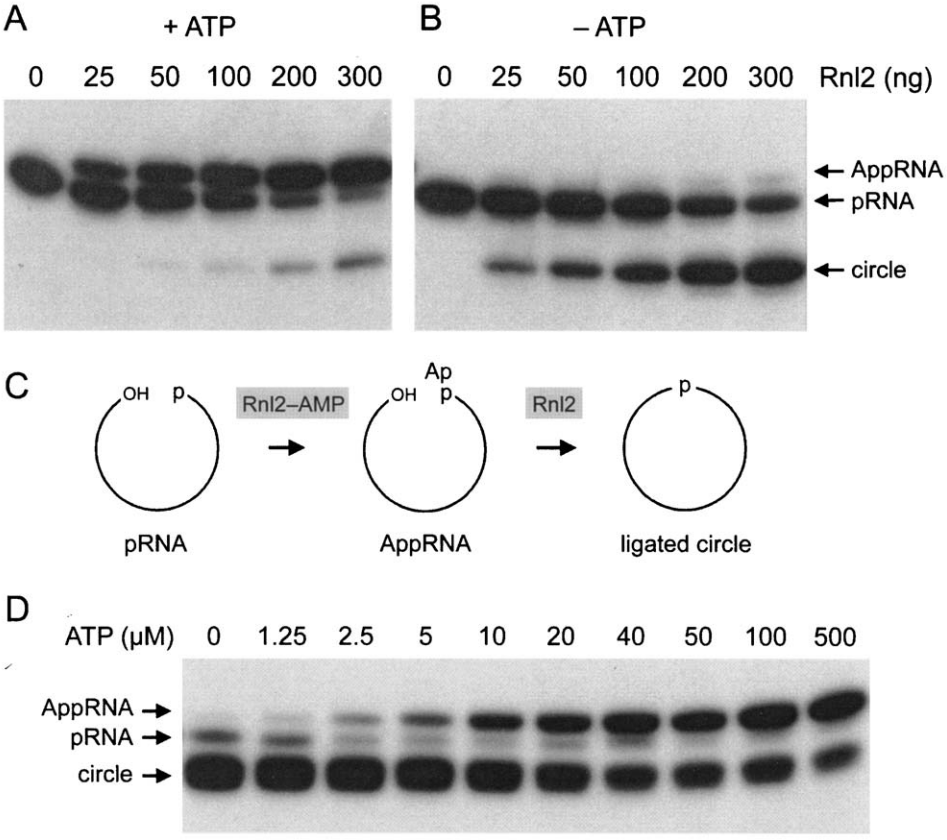

Fig. 5. RNA ligase activity and effect of ATP on RNA–adenylate formation by KVP40 Rnl2. The reaction products were analyzed by denaturing PAGE. RNA ligase activity is demonstrated in panels A and B. The step 2 (RNA adenylation) and step 3 (phosphodiester bond formation) reactions of the ligation pathway are illustrated schematically in panel C. Reaction mixtures (10 μl) containing 50 mM Tris–HCl (pH 7.0), 5 mM DTT, 3 mM $MgCl_2$, 1 pmol of 5′ ^{32}P-labeled 18-mer RNA, and either 1 mM ATP (panel A) or no ATP (panel B), and 0, 25, 50, 100, 200, or 300 ng Rnl2 (i.e., 0, 0.6, 1.3, 2.5, 5, or 7.5 pmol Rnl2) were incubated for 30 min at 22°C. The reaction products were analyzed by PAGE and visualized by autoradiography. The positions of the labeled 18-mer substrate strand (pRNA), the ligated 18-mer circle, and the RNA–adenylate intermediate (AppRNA) are indicated by arrows on the *right*. (D) ATP titration. Reaction mixtures (10 μl) containing 50 mM Tris–HCl (pH 7.0), 5 mM DTT, 3 mM $MgCl_2$, 1 pmol of 5′ ^{32}P-labeled 18-mer RNA, 200 ng (5 pmol) Rnl2, and ATP as specified were incubated for 30 min at 22°C.

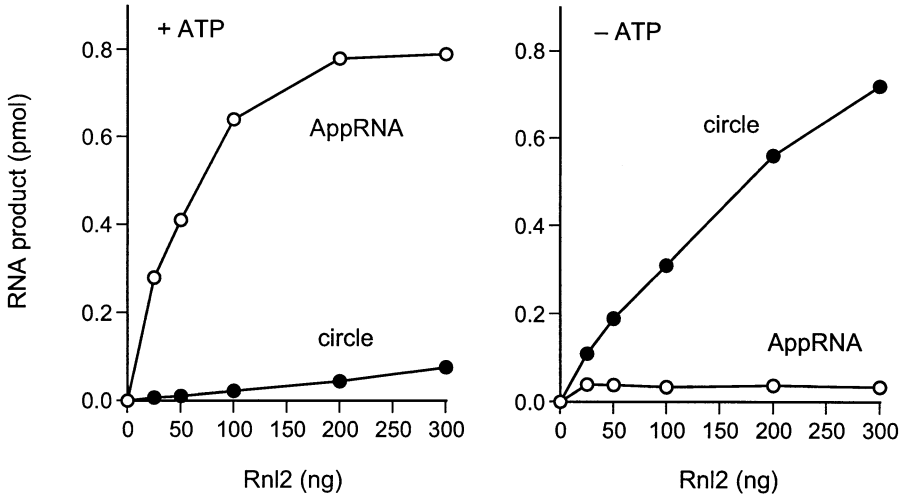

Fig. 6. Ligase specific activity of KVP40 Rnl2. The amounts of AppRNA and circular RNA products formed in the reactions shown in Figs. 5A and B were quantitated by scanning the gel with a phosphorimager and are plotted as a function of input Rnl2.

RNA–adenylate intermediate

A kinetic analysis of the strand-joining reaction in the absence of ATP showed that RNA–adenylate was the first product formed by KVP40 Rnl2 (Fig. 7A). RNA–adenylate was visible at 1 min (at which point no circular RNA was seen) and persisted from 1 to 8 min before declining, concomitant with decay of the 18-mer pRNA substrate and steady accumulation of ligated circle (Fig. 7A). These results suggest that the RNA–adenylate is a genuine intermediate along the Rnl2 strand-joining pathway. The kinetic experiment was performed at a concentration of Rnl2–AMP (~170 nM) in excess of the concentration of pRNA substrate (100 nM), thereby accounting for the high extent of ATP-independent circularization. The relatively low amount of AppRNA intermediate present at early times suggested that the rate of step 3 (circularization of AppRNA) was greater than the rate of step 2 (AMP transfer from Rnl2–AMP to pRNA). The slow overall reaction (which attained 50% of the endpoint after 8–10 min) may reflect a rate-limiting binding step at nanomolar levels of enzyme and pRNA.

Additional evidence implicating RNA–adenylate as a reaction intermediate emerged from an analysis of pH effects on the strand-joining reaction in the absence of ATP (Fig. 7B). The yield of the circular product was optimal

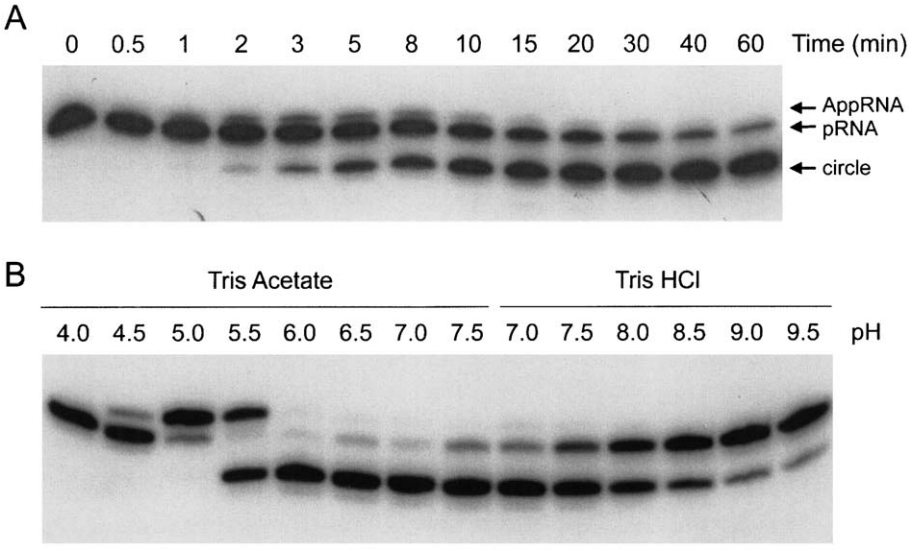

Fig. 7. Kinetics and pH dependence of the pRNA ligation reaction of KVP40 Rnl2. (A) Kinetics. A reaction mixture (140 μl) containing 50 mM Tris–HCl (pH 7.0), 5 mM DTT, 3 mM $MgCl_2$, 14 pmol 5′ ^{32}P-labeled 18-mer RNA, and 5.6 μg (140 pmol) Rnl2 was incubated at 22°C. Aliquots (10 μl) were withdrawn at the times indicated and quenched immediately with formamide–EDTA. (B) pH dependence. Reaction mixtures (20 μl) containing 50 mM buffer (either Tris–acetate pH 4.0, 4.5, 5.0, 5.5, 6.0, 6.5, 7.0, or 7.5 or Tris–HCl pH 7.0, 7.5, 8.0, 8.5, 9.0, or 9.5), 5 mM DTT, 3 mM $MgCl_2$, 1 pmol 5′ ^{32}P-labeled 18-mer RNA, and 400 ng (10 pmol) Rnl2 were incubated for 30 min at 22°C.

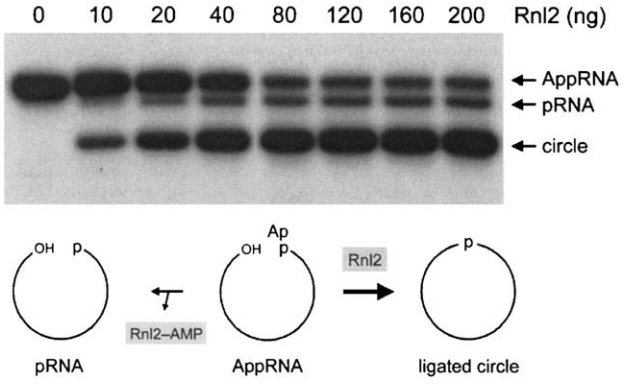

Fig. 8. Ligation of a preadenylated RNA substrate by KVP40 Rnl2. The 5′ adenylated ^{32}P-labeled 18-mer RNA strand (AppRNA) was synthesized and gel-purified as described under Experimental procedures. The two potential reactions of Rnl2 with the isolated AppRNA are illustrated schematically: Step 3 entails attack in *cis* of the 3′-OH on the RNA adenylate to form a circular RNA product; step −2 (reverse of step 2) is the transfer of AMP from RNA–adenylate to the ligase to form a linear 5′ phosphate RNA. Reaction mixtures (10 μl) containing 50 mM Tris–HCl (pH 7.0), 5 mM DTT, 3 mM $MgCl_2$, 0.16 pmol of ^{32}P-labeled AppRNA, and Rnl2 as specified were incubated for 30 min at 22°C. The products were resolved by PAGE and visualized by autoradiography. The positions of the labeled AppRNA substrate, the ligated 18-mer circle, and the deadenylated pRNA are indicated by arrows on the *right*.

between pH 6.0 and 7.0. Reducing the pH to 5.0 completely suppressed the formation of circles, but stimulated the formation of RNA–adenylate. This result implies that the step of phosphodiester bond formation became rate-limiting at pH 5.0–5.5, so that the RNA–adenylate intermediate accumulated to high levels. Further reduction of the pH to 4.0 abolished all activity of KVP40 Rnl2. Raising the pH to ≥8.0 suppressed the intramolecular ligation reaction, but did not result in accumulation of AppRNA (Fig. 7B).

Phosphodiester formation at a pre-adenylated RNA 5′ end

We synthesized and gel-purified a pre-adenylated 18-mer RNA substrate for analysis of the isolated step 3 reaction of KVP40 Rnl2. Formation of a phosphodiester at the activated 5′ end was evinced by the appearance of a sealed circular RNA product, the yield of which was proportional to the amount of input Rnl2 (Fig. 8). Seventy-eight percent of the substrate was converted to circular RNA at saturating Rnl2 concentrations. Eleven percent of the input AppRNA was deadenylated to yield pRNA, which migrated between RNA–adenylate substrate and the ligated circle (Fig. 8). Deadenylation is the reverse of step 2 of the ligation pathway.

Effect of pRNA length on strand joining by Rnl2

The above characterization of KVP40 Rnl2 indicates that it resembles T4 Rnl2 in most respects. To extend our understanding of the strand-joining properties of the phage Rnl2 enzymes, we examined the effect of pRNA length on

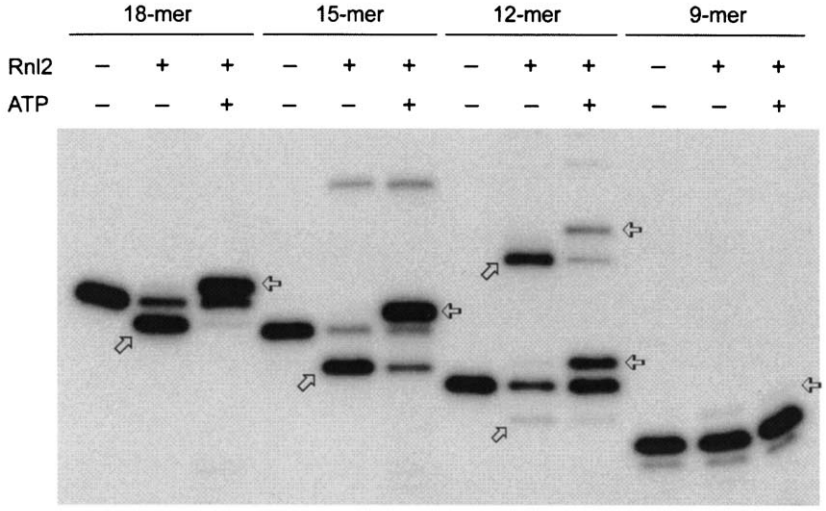

Fig. 9. Effect of RNA length on strand-joining activity of T4 Rnl2. Reaction mixtures (10 μl) containing 50 mM Tris–acetate (pH 6.5), 5 mM DTT, 1 mM $MgCl_2$, 1 pmol 5′ ^{32}P-labeled 18-mer, 15-mer, 12-mer, or 9-mer RNAs as specified, 320 ng (8 pmol) T4 Rnl2, and either 1 mM ATP (+ATP) or no ATP (−ATP) were incubated for 15 min at 22°C. The products were resolved by PAGE and visualized by autoradiography. Rnl2 was omitted from the control reaction mixture in lane −. Circular reaction products are denoted by ⇗. RNA adenylate products are indicated by ⇦ The sequences of the RNA substrates are shown at the *bottom*.

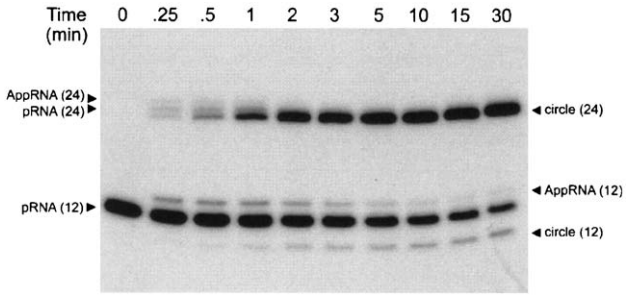

Fig. 10. Kinetic analysis of 12-mer pRNA ligation by T4 Rnl2. A reaction mixture (100 μl) containing 50 mM Tris–acetate (pH 6.5), 5 mM DTT, 1 mM $MgCl_2$, 10 pmol of 5′ ^{32}P-labeled 12-mer pRNA substrate, and 800 ng (20 pmol) of T4 Rnl2 were incubated at 22°C. Aliquots (10 μl) were withdrawn at the times indicated and quenched immediately with formamide–EDTA. The products were resolved by PAGE and visualized by autoradiography. The positions of the 18-mer pRNA substrate, 24-mer pRNA dimer, and 24-mer RNA adenylate are indicated on the *left*. The monomer circle, monomer RNA adenylate, and dimer circle products are indicated on the *right*.

the reactivity and product distribution of T4 Rnl2 (Fig. 9). The reaction of T4 Rnl2 with an 18-mer pRNA generated an 18-mer circle in the absence of ATP (denoted by ⇗) and an 18-mer AppRNA in the presence of ATP (indicated by ⇦). Shortening the input pRNA strand to 15 nucleotides did not affect the overall extent of conversion of the substrate to products, which were predominantly a 15-mer circle in the absence of ATP and a 15-mer AppRNA in the presence of ATP. However, low levels of dimeric ligation products were also detectable.

Shortening the pRNA substrate to 12 nucleotides elicited a clear shift in product distribution to predominantly dimer circles in the absence of ATP, with only trace production of monomer circles (Fig. 9). Thus, the enzyme switches to an intermolecular reaction from an intramolecular process with the 12-mer pRNA. A kinetic analysis of the reaction of Rnl2–AMP with the 12-mer pRNA is shown in Fig. 10. Initial AMP transfer from Rnl2–AMP to the 12-mer pRNA results in formation of 12-mer AppRNA within 15 s; also detectable at this time is a cluster of three larger species corresponding to 24-mer linear pRNA dimer, 24-mer AppRNA dimer, and 24-mer circular dimer (Fig. 10). The dimer linear pRNA and dimer RNA–adenylate species declined by 2 min as ligated dimer circle began to accumulate, concomitant with consumption of the input 12-mer pRNA (Fig. 10). Formation of dimer circles was suppressed when Rnl2 reacted with the 12-mer pRNA in the presence of ATP, which resulted in trapping of the 12-mer AppRNA and 24-mer AppRNA species as the major and minor products, respectively (Fig. 9). We construe that the 12-mer pRNA is too short to simultaneously occupy the 5′ -PO_4 and 3′ -OH binding pockets at the Rnl2 active site.

T4 Rnl2 was incapable of ligating a 9-mer pRNA substrate, either intramolecularly or intermolecularly (Fig. 9). Because only trace amounts of adenylated 9-mer RNA were detected in the presence of ATP, we surmise that Rnl2 requires a minimum RNA length to activate the 5′ -PO_4 of the "donor" strand. KVP40 Rnl2 was also unreactive with the 9-mer pRNA substrate (not shown).

Effect of the terminal nucleoside sugar on strand joining by T4 Rnl2

Whereas bacteriophage T4 Rnl2 readily circularizes an 18-mer pRNA strand, it is completely unreactive with an 18-mer pDNA strand of identical base sequence (Ho and Shuman, 2002). To investigate the basis for the RNA specificity of T4 Rnl2, we tested its activity with two 18-mer substrates composed of 17 contiguous ribonucleotides plus a single deoxyribonucleotide at either the 5′ or 3′ end (Fig. 11). The 5′ deoxy-terminated pRNA substrate was efficiently circularized by Rnl2–AMP in the absence of exogenous ATP (Fig. 11A, top panel). As with the all-RNA substrate, we detected a transient 5′ -adenylated polynucleotide intermediate (designated AppRNA*) at early times in the course of the reaction. Inclusion of ATP precluded circularization and trapped the 5′ -adenylated nucleic acid (Fig. 11A, bottom panel). The rates of formation of the adenylated and circular products with the 5′ deoxy-terminated pRNA substrate were similar to those seen for an all-RNA substrate (Ho and

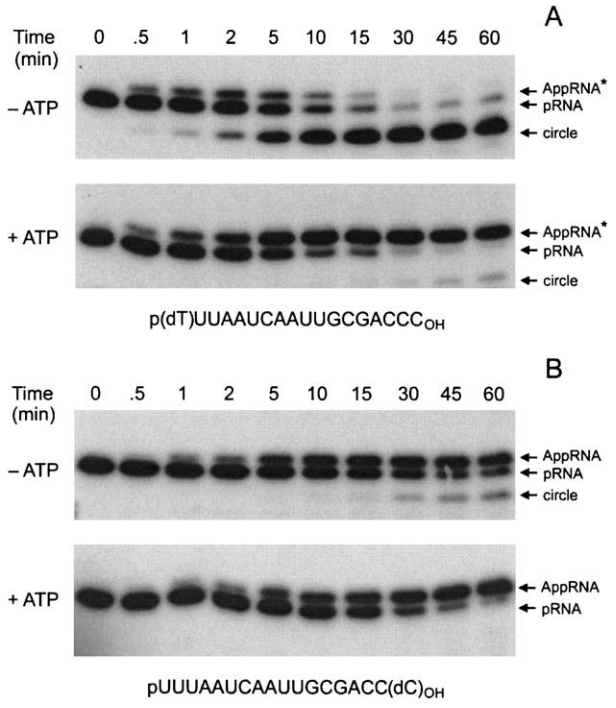

Fig. 11. Effect of the terminal nucleoside sugar on strand joining by T4 Rnl2. A reaction mixture (100 μl) containing 50 mM Tris–acetate (pH 6.5), 5 mM DTT, 1 mM $MgCl_2$, either no added ATP or 1 mM ATP as specified, 10 pmol of 5′ ^{32}P-labeled 5′ deoxy-substituted pRNA substrate (panel A) or 3′ deoxy-substituted pRNA (panel B), and 800 ng (20 pmol) of T4 Rnl2 were incubated at 22°C. Aliquots (10 μl) were withdrawn at the times indicated and quenched immediately with formamide–EDTA. The products were resolved by PAGE and visualized by autoradiography.

Shuman, 2002). Thus, Rnl2 was able to transfer AMP to a 5′ deoxyribonucleotide end and to catalyze attack of a ribonucleotide 3′ -OH on the App(dN) intermediate to form a mixed 5′ -(rN′)p(dN) phosphodiester.

In contrast, the introduction of a single 3′ deoxyribonucleotide strongly suppressed the ATP-independent circularization reaction and resulted in the accumulation of high levels of AppRNA that persisted for up to 60 min (Fig. 11B, top panel). Inclusion of ATP eliminated what little circularization did occur in its absence and again resulted in trapping of high levels of AppRNA (Fig. 11B, bottom panel). These results show that a 3′ ribonucleotide is critical for efficient phosphodiester bond formation (step 3), but not for the 5′ adenylylation step (step 2) of the ligation pathway. Note, however, that although the yield of the 5′ -adenylated end was as high with the 3′ deoxy pRNA substrate as with the 5′ deoxy pRNA (compare bottom panels in A and B), quantitation of the products as a function of time showed that the rate of the RNA adenylation reaction was 3-fold slower with the 3′ deoxy substrate. Similar effects of 5′ and 3′ deoxy substitutions on product distribution were observed with KVP40 Rnl2 (not shown).

Discussion

Here we show that vibriophage KVP40 encodes an RNA strand-joining enzyme that is structurally and biochemically homologous to T4 Rnl2. The vibriophage and coliphage Rnl2–AMP complexes act stoichiometrically in the absence of added ATP to convert linear pRNAs into covalently closed monomeric RNA circles. In contrast, the reaction of KVP40 and T4 Rnl2 with single-strand RNAs of ≥12-nucelotides in the presence of ATP results in ‘‘capping’’ of the RNA 5′ end with AMP to form AppRNA. As noted above, this effect is likely caused by dissociation of Rnl2 from newly formed AppRNA followed immediately by ligase adenylation, which precludes the third step of the strand-joining pathway. Phosphodiester bond formation by Rnl2 was also impeded by a single deoxyribose sugar substitution at the 3′ end of the pRNA substrate. In the case of T4 RNA ligase 1, Sugino et al. (1977) showed that the 5′ RNA adenylylation and end-sealing steps were both blocked by periodate oxidation of the 3′ terminal ribose of the RNA substrate, which converts the 3′ ribose sugar into a ring-opened 2′ ,3′ dialdehyde. Although T4 Rnl1 displays relatively feeble activity in sealing oligodeoxyribonucleotide substrates (Hinton et al., 1978; Sugino et al., 1977), the reaction of T4 Rnl1 with DNA is notable for the accumulation of high levels of the 5′ adenylated nucleic acid intermediate (Sugino et al., 1977). Collectively, the studies of Rnl1 and Rnl2 suggest a general theme that the 2′ -sugar substituent at the 3′ terminus participates in the RNA sealing step, either by promoting recognition of the reactive 3′ -OH end or the chemistry of the step 3 reaction.

The biochemical properties of the phage Rnl2 enzymes raise interesting questions about the kinds of reactions they might catalyze in a cellular milieu where ATP is present at millimolar concentrations. We focus our speculations on two possible scenarios. In the first case, we envision that the biological function of Rnl2 is indeed ATP-dependent RNA strand joining and we posit that Rnl2 either recognizes a specific RNA structure, from which it would not dissociate after the RNA adenylation step, or it requires a partner protein that anchors it to RNA adenylate to promote immediate completion of the sealing step. Previous studies indicated that the ATP effect on trapping of RNA adenylate is not prevented when T4 Rnl2 reacts with a stem–loop RNA designed to mimic the broken tRNA anticodon stem–loop that serves as the in vivo substrate for T4 Rnl1 (Yin et al., 2003). Studies of the kinetoplastid RNA-editing ligases (which we classify as Rnl2-like enzymes) do indicate that the RELs prefer to join RNA termini that are splinted together by a bridging RNA template strand (Blanc et al., 1999; Palazzo et al., 2003). It is notable that the specificity for RNA versus DNA as the template bridge differed between recombinant REL and the REL present in the native ‘‘editosome’’ complex, suggesting that editosome components associated with REL can alter its substrate preference (Palazzo et al., 2003). In this light, it will be of interest to compare the properties of recombinant phage Rnl2 with native Rnl2 isolated from KVP40-infected or T4-infected bacteria.

A second possible scenario is that Rnl2 actually does function to adenylate pRNA ends in vivo. 5′ Monophosphate-terminated substrates for Rnl2 could be generated either by endonucleolytic cleavage or by the removal of the γ and β phosphates from the 5′ triphosphate ends of primary transcripts. A blocked 5′ AppRNA terminus could potentially influence the stability of host or phage-derived RNAs and, in the case of mRNAs, affect their efficiency of translation. It is conceivable that a 5′ AppRNA end could facilitate translation of a 5′ leaderless transcript lacking a Shine-Dalgarno sequence (O’Donnell and Janssen, 2002).

ATP-dependent synthesis of AppRNA by bacteriophage Rnl2 is reminiscent of the capping of eukaryotic mRNA by GTP:RNA guanylyltransferase. This functional connection between Rnl2 and capping enzymes, together with previous mutational studies highlighting the similarities of the active sites of T4 Rnl2 and RNA guanylyltransferase (Yin et al., 2003), suggests an evolutionary link between bacteriophage Rnl2 and eukaryotic RNA capping enzymes. Capping enzymes modify the 5′ diphosphate terminus of single-stranded RNA substrates by transfer of GMP from GTP to the RNA β phosphate through a covalent enzyme–GMP intermediate (Shuman and Hurwitz, 1981). If it is the case that capping enzymes evolved from an ancestral RNA ligase, the properties of phage Rnl2 may represent an intermediate step in that process, whereby Rnl2 has diminished capacity to join strands in the presence of the NTP substrate and prefers to synthesize an inverted NMP-

(5′)-(5′)-RNA product. The intervening stages between Rnl2 and capping enzymes would entail the acquisition of specificity for GTP over ATP in the formation of the enzyme–NMP intermediate and the acquisition of preference for a 5′ diphosphate RNA end.

Experimental procedures

KVP40 Rnl2

KVP40 ORF293 was amplified by PCR from KVP40 DNA with primers designed to introduce an *Nde*I restriction site at the start codon and a *Bam*HI site 3′ of the stop codon. The PCR product was digested with *Nde*I and *Bam*HI and inserted into pET16b (Novagen) to generate the plasmid pET-kRNL2 encoding the KVP40 polypeptide fused to an N-terminal His_{10} tag. The insert was sequenced completely to exclude the acquisition of unwanted changes during amplification and cloning. pET-kRNL2 was transformed into *E. coli* BL21(DE3). A 1-l culture of *E. coli* BL21(DE3)/pET-kRNL2 was grown at 37°C in LB medium containing 0.1 mg/ml ampicillin until the A_{600} reached 0.5. The culture was adjusted to 0.5 mM isopropyl-β-D-thiogalactoside (IPTG) and incubation was continued at 37°C for 3 h. Cells were harvested by centrifugation and the pellet was stored at −80°C. All subsequent procedure were performed at 4°C. Thawed bacteria were resuspended in 20 ml of buffer A [50 mM Tris–HCl (pH 7.5), 0.2 M NaCl, 10% sucrose]. Lysozyme and Triton X-100 were added to final concentrations of 50 μg/ml and 0.1%, respectively. The lysate was sonicated to reduce viscosity and insoluble material was removed by centrifugation. The soluble extract was applied to a 2-ml column of Ni–NTA agarose (Qiagen, Chatsworth, CA) that had been equilibrated with buffer A containing 0.1% Triton X-100. The column was washed with 20 ml of the same buffer and then eluted stepwise with 3-ml aliquots of 50, 100, 200, and 500 mM imidazole in buffer B [50 mM Tris–HCl (pH 8.0), 0.2 M NaCl, 10% glycerol, 0.05% Triton X-100]. The polypeptide composition of the column fractions was monitored by SDS-PAGE. KVP40 Rnl2 was recovered predominantly in the 200 mM imidazole eluate, which was dialyzed against buffer containing 50 mM Tris–HCl (pH 8.0), 0.1 M NaCl, 1 mM DTT, 10% glycerol, 0.05% Triton X-100. The Rnl1 preparation was stored at −80°C. Protein concentration was determined with the Bio-Rad dye reagent using bovine serum albumin as the standard.

Adenylyltransferase assay

Reaction mixtures (20 μl) containing 50 mM Tris–acetate (pH 7.0), 5 mM DTT, 3 mM $MgCl_2$, 20 μM [α-^{32}P]ATP, and Rnl2 as specified were incubated for 5 min at 37°C. The reactions were quenched with SDS and the products were analyzed by SDS-PAGE. The ligase–[^{32}P]AMP adduct was visualized by autoradiography of the dried gel and quantitated by scanning the gel with a phosphorimager.

RNA ligase assay

An 18-mer oligoribonucleotide (5′ -UUUAAUCAAUU-GCGACCC; purchased from Dharmacon) was 5′ ^{32}P-labeled using T4 polynucleotide kinase and [γ-^{32}P]ATP and then purified by electrophoresis through a nondenaturing 18% polyacrylamide gel. Additional RNA oligoribonucleotides and deoxy-substituted oligoribonucleotides as specified were purchased from Dharmacon and 5′ ^{32}P-labeled in the same fashion. RNA ligation reaction mixtures (10 μl) containing 50 mM Tris–HCl (pH 7.0), 5 mM DTT, 3 mM $MgCl_2$, 1 pmol of 5′ ^{32}P-labeled RNA, and ATP and Rnl2 as specified were incubated for 30 min at 22°C. The reactions were quenched by adding 5 μl of 90% formamide, 20 mM EDTA. The samples were analyzed by electrophoresis through an 18% polyacrylamide gel containing 7 M urea in 45 mM Tris–borate, 1 mM EDTA. The ligation products were visualized by autoradiography and quantitated by scanning the gel with a phosphorimager.

Preparation of RNA–adenylate

Two nanomoles of ^{32}P-labeled 18-mer RNA was incubated with 50 μg of purified T4 Rnl2 in the presence of 1 mM ATP and 7.5 mM $MgCl_2$ for 30 min at 22°C. The products were then treated with 25 U of calf intestine alkaline phosphatase (Roche Bioscience) for 60 min at 37°C and resolved by electrophoresis through a native 18% polyacrylamide gel in 90 mM Tris–borate, 2 mM EDTA. The ^{32}P-labeled AppRNA strand was located by autoradiography of the wet gel and then eluted from an excised gel slice in 10 mM Tris–HCl (pH 8.0), 1 mM EDTA.

References

Amitsur, M., Levitz, R., Kaufman, G., 1987. Bacteriophage T4 anticodon nuclease, polynucleotide kinase, and RNA ligase reprocess the host lysine tRNA. EMBO J. 6, 2499–2503.

Baymiller, J., Jennings, S., Kienzle, B.K., Gorman, J.A., Kelly, R., McCullough, J.E., 1994. Isolation and sequence of the tRNA ligase-encoding gene of *Candida albicans*. Gene 142, 129–134.

Blanc, V., Alfonso, J.D., Aphasizhev, R., Simpson, L., 1999. The mitochondrial RNA ligase from *Leishmania tarentolae* can join RNA molecules bridged by a complementary RNA. J. Biol. Chem. 274, 24289–24296.

Cranston, J.W., Silber, R., Malathi, V.G., Hurwitz, J., 1974. Studies on ribonucleic acid ligase: characterization of an adenosine triphosphate–inorganic pyrophosphate exchange reaction and demonstration of an enzyme–adenylate complex with T4 bacteriophage-induced enzyme. J. Biol. Chem. 249, 7447–7456.

Durantel, D., Croizier, L., Ayres, M.D., Croizier, G., Possee, R.D., Lopez-Ferber, M., 1998. The pnk/pnl gene (ORF 86) of *Autographa californica* nucleopolyhedrovirus is a noon-essential, immediate early gene. J. Gen. Virol. 79, 629–637.

Fabrega, C., Shen, V., Shuman, S., Lima, C.D., 2003. Structure of an mRNA capping enzyme bound to the phosphorylated carboxyl-terminal domain of RNA polymerase II. Mol. Cell 11, 1549–1561.

Håkansson, K., Doherty, A.J., Shuman, S., Wigley, D.B., 1997. X-ray crystallography reveals a large conformational change during guanyl transfer by mRNA capping enzymes. Cell 89, 545–553.

Hinton, D.M., Baez, J.A., Gumport, R.I., 1978. T4 RNA ligase joins 2′ -deoxyribonucleoside 3′ ,5′ -bisphosphates to oligodeoxyribonucleotides. Biochemistry 17, 5091–5097.

Ho, C.K., Shuman, S., 2002. Bacteriophage T4 RNA ligase 2 (gp24.1) exemplifies a family of RNA ligases found in all phylogenetic domains. Proc. Natl. Acad. Sci. U.S.A. 99, 12709–12714.

Lee, J.Y., Chang, C., Song, H.K., Moon, J., Yang, J., Kim, H.K., Kwon, S.T., Suh, S.W., 2000. Crystal structure of NAD^+-dependent DNA ligase: modular architecture and functional implications. EMBO J. 19, 1119–1129.

McManus, M.T., Shimamura, M., Grams, J., Hajduk, S.L., 2001. Identification of candidate mitochondrial RNA editing ligases from *Trypanosoma brucei*. RNA 7, 167–175.

Miller, E.S., Heidelberg, J.F., Eisen, J.A., Nelson, W.C., Durkin, A.S., Ciecko, A., Feldlyum, T.V., White, O., Paulsen, I.T., Nierman, W.C., Lee, J., Szcypinski, B., Fraser, C.M., 2003a. Complete genome sequence of the broad-host-range vibriophage KVP40: comparative genomics of a T4-related bacteriophage. J. Bacteriol. 185, 5220–5233.

Miller, E.S., Kutter, E., Mosig, G., Arisaka, F., Kunisawa, T., Rüger, W., 2003b. Bacteriophage T4 genome. Microbiol. Mol. Biol. Rev. 67, 86–156.

Odell, M., Sriskanda, V., Shuman, S., Nikolov, D., 2000. Crystal structure of eukaryotic DNA ligase–adenylate illuminates the mechanism of nick sensing and strand joining. Mol. Cell 6, 1183–1193.

O'Donnell, S.M., Janssen, G.R., 2002. Leaderless mRNAs bind 70S ribosomes more strongly that 30S ribosomal subunits in *Escherichia coli*. J. Bacteriol. 184, 6730–6733.

Palazzo, S.S., Panigrahi, A.K., Igo, R.P., Salavati, R., Stuart, K., 2003. Kinetoplastid RNA editing ligases: complex association, characterization, and substrate requirements. Mol. Biochem. Parasitol. 127, 161–167.

Phizicky, E.M., Schwartz, R.C., Abelson, J., 1986. *Saccharomyces cerevisiae* tRNA ligase: purification of the protein and isolation of the structural gene. J. Biol. Chem. 261, 2978–2986.

Rusche, L.N., Huang, C.E., Piller, K.J., Hemann, M., Wirtz, E., Sollner-Webb, B., 2001. The two RNA ligases of the *Trypanosoma brucei* RNA editing complex: cloning of the essential band IV gene and identifying the band V gene. Mol. Cell. Biol. 21, 979–989.

Sawaya, R., Schwer, B., Shuman, S., 2003. Genetic and biochemical analysis of the functional domains of yeast tRNA ligase. J. Biol. Chem. 278, 43298–43398.

Schnaufer, A., Panigrahi, A.K., Panicucci, B., Igo, R.P., Salavati, R., Stuart, K., 2001. An RNA ligase essential for RNA editing and survival of the bloodstream form of *Trypanosoma brucei*. Science 291, 2159–2162.

Shuman, S., 2000. Structure, mechanism, and evolution of the mRNA capping apparatus. Prog. Nucleic Acid Res. Mol. Biol. 66, 1–40.

Shuman, S., Hurwitz, J., 1981. Mechanism of mRNA capping by vaccinia virus guanylyltransferase: characterization of an enzyme–guanylate intermediate. Proc. Natl. Acad. Sci. U.S.A. 78, 187–191.

Shuman, S., Schwer, B., 1995. RNA capping enzyme and DNA ligase—A superfamily of covalent nucleotidyl transferases. Mol. Microbiol. 17, 405–410.

Silber, R., Malathi, V.G., Hurwitz, J., 1972. Purification and properties of bacteriophage T4-induced RNA ligase. Proc. Natl. Acad. Sci. U.S.A. 69, 3009–3013.

Subramanya, H.S., Doherty, A.J., Ashford, S.R., Wigley, D.B., 1996. Crystal structure of an ATP-dependent DNA ligase from bacteriophage T7. Cell 85, 607–615.

Sugino, A., Snopek, T.J., Cozzarelli, N.R., 1977. Bacteriophage T4 RNA ligase: reaction intermediates and interaction of substrates. J. Biol. Chem. 252, 1732–1738.

Thogersen, H.C., Morris, H.R., Rand, K.N., Gait, M.J., 1985. Location of the adenylylation site in T4 RNA ligase. Eur. J. Biochem. 147, 325–329.

Tomkinson, A.E., Totty, N.F., Ginsburg, M., Lindahl, T., 1991. Location of the active site for enzyme–adenylate formation in DNA ligases. Proc. Natl. Acad. Sci. U.S.A. 88, 400–404.

Uhlenbeck, O.C., Gumport, R.I., 1982. RNA ligase. The Enzymes 15, 31–58.

Wang, L.K., Ho, C.K., Pei, Y., Shuman, S., 2003. Mutational analysis of bacteriophage T4 RNA ligase 1: different functional groups are required for the nucleotidyl transfer and phosphodiester bond formation steps of the ligation reaction. J. Biol. Chem. 278, 29454–29462.

Xu, Q., Teplow, D., Lee, T.D., Abelson, J., 1990. Domain structure in yeast tRNA ligase. Biochemistry 29, 6132–6138.

Yin, S., Ho, C.K., Shuman, S., 2003. Structure–function analysis of T4 RNA ligase 2. J. Biol. Chem. 278, 17601–17608.